Dexter, R.J. and Fisher, J.W. “Fatigue and Fracture”
Structural Engineering Handbook
Ed. Chen Wai-Fah
Boca Raton: CRC Press LLC, 1999

Fatigue and Fracture

Robert J. Dexter and
John W. Fisher
Department of Civil Engineering, Lehigh University, Bethlehem, PA

24.1 Introduction

This chapter provides an overview of aspects of fatigue and fracture that are relevant to design or assessment of structural components made of concrete, steel, and aluminum. This chapter is intended for practicing civil and structural engineers engaged in regulation, design, inspection, repair, and retrofit of a variety of structures ,including buildings; bridges; sign, signal, and luminaire support structures; chimneys; transmission towers ;et c. Established procedures are explained for design and in-service assessment to ensure that structures are resistant to fatigue and fracture. This chapter is not intended as a comprehensive review of the latest research results in the subject area; therefore, many interesting aspects of fatigue and fracture are not discussed.

The design and assessment procedures outlined in this chapter maybe applied to other similar structures, even outside the traditional domain of civil engineers, including offshore structures, cranes, heavy vehicle frames, and ships. The mechanical engineering approach, which works well for smooth machine parts, gives an overly optimistic assessment of the fatigue strength of structural details. There are many cases of failures of these types of structures, such as the crane in Figure24.1 or the vehicle frame in Figure24.2, which would have been predicted had the structural engineering approach been applied.

The possibility of fatigue must be checked for any structural member that is subjected to cyclic loading. Among the few cases where cracking has occurred in structures, the cracks are usually only a nuisance and may even go unnoticed. Only in certain truly non-redundant structural systems can cracking lead to structural collapse. The loading for most structures is essentially under fixed- can cracking lead to structural collapse. The loading for most structures is essentially under fixed- connections in redundant structures are essentially under displacement-control boundary conditions. In other words, because of the stiffness of the surrounding structure, the ends of the member have to

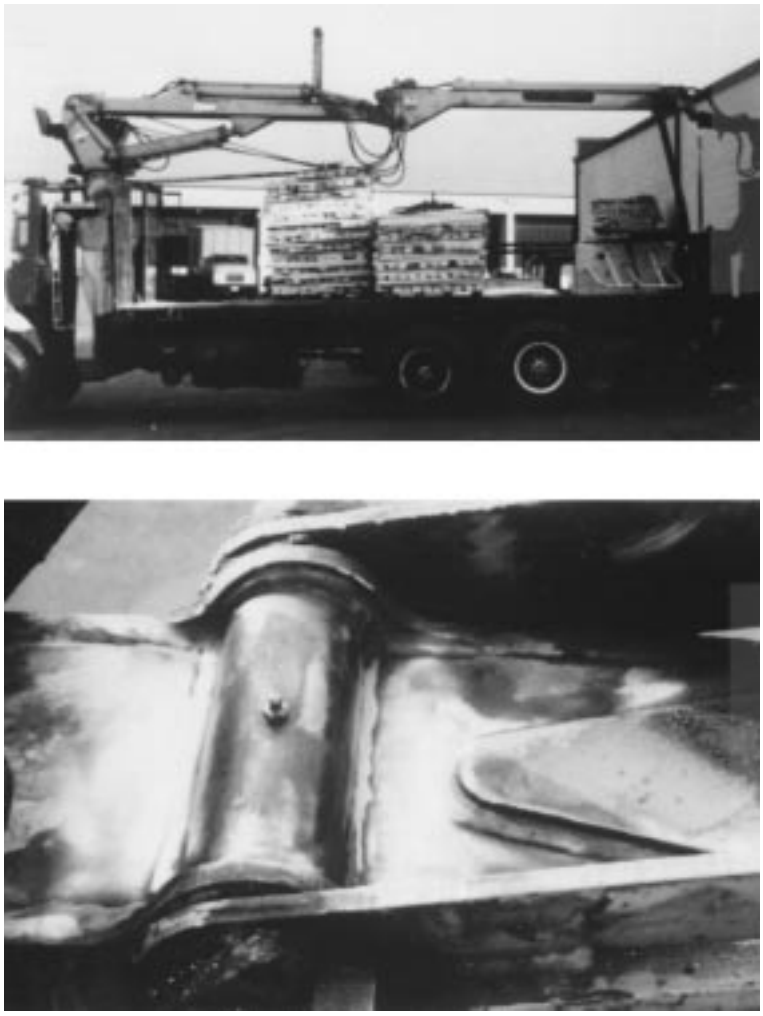

FIGURE 24.1: Fatigue cracking at welded detail in crane boom.

deform in a way that is compatible with nearby members. Under displacement control, a member can continue to provide integrity (e.g., transfer shear) after it has reached ultimate strength and is in the descending branch of the load-displacement curve. This behavior under displacement control is referred to as load shedding. In order for load shedding to be fully effective, individual critical members in tension must elongate to several times the yield strain locally without completely fracturing.

Good short-term performance should not lead to complacency, because fatigue and stress-corrosion cracking may take decades to manifest. Corrosion and other structural damage can precipitate and accelerate fatigue and fracture. Also, fabrication cracks may be built into a structure and never discovered. These dormant cracks can fracture if the structure is ever loaded into the inelastic range, such as in an earthquake.

Fatigue cracking in steel bridges in the U.S. has become a more frequent occurrence since the 1970s. Figure 24.3 shows a large crack that was discovered in 1970 at the end of a coverplate in one of the Yellow Mill Pond multibeam structures located at Bridgeport, Connecticut. Between 1970 and 1981,

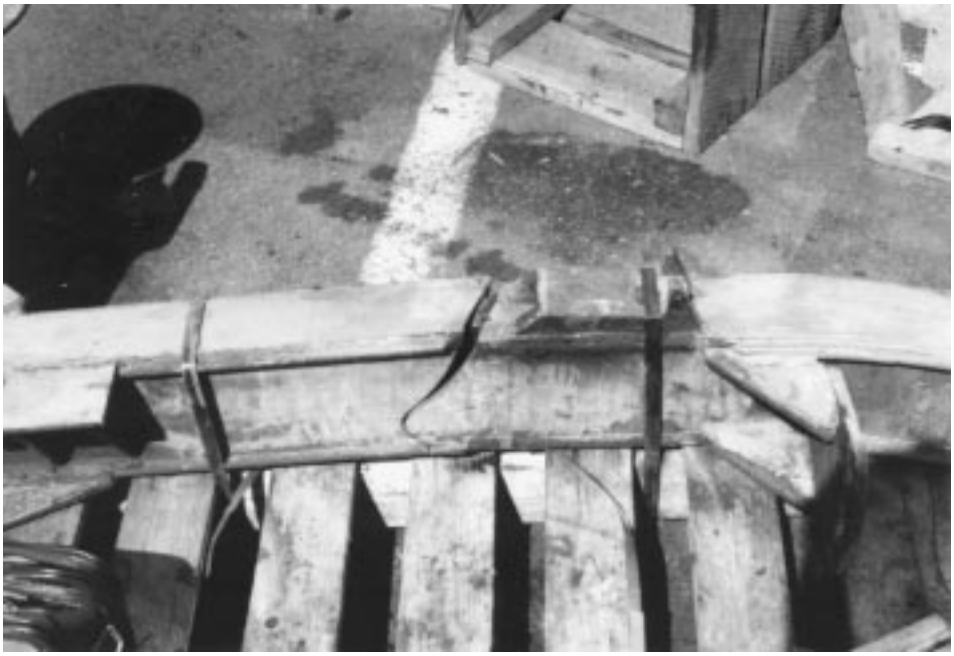

FIGURE 24.2: Fatigue cracking at welded detail in vehicle frame.

numerous fatigue cracks were discovered at the ends of coverplates in this bridge [19].

Fatigue cracking in bridges, such as shown in Figure 24.3, resulted from an inadequate experimental base and overly optimistic specification provisions developed from the experimental data in the 1960s. The assumption of a fatigue limit at two million cycles proved to be incorrect. As a result of extensive large-scale fatigue testing, it is now possible to clearly identify and avoid details that are expected to have low fatigue strength. The fatigue problems with the older bridges can be avoided in new construction. Fortunately, it is also possible to retrofit or upgrade the fatigue strength of existing bridges with poor details.

Low-cycle fatigue is a possible failure mode for structural members or connections that are cycled into the inelastic region for a small number of cycles. For example, bracing members in a braced frame or beam-to-column connections in a welded special-moment frame (WSMF) may be subjected to low-cycle fatigue in an earthquake. In sections that are cyclically buckling, the low-cycle fatigue is linked to the buckling behavior. This emerging area of research is briefly discussed in Section 24.2.5.

The primary emphasis in this chapter is on high-cycle fatigue. Truck traffic causes high-cycle fatigue of bridges. Fatigue cracking may occur in industrial buildings subjected to loads from cranes or other equipment or machinery. Although it has not been a problem in the past, fatigue cracking could occur in high-rise buildings frequently subjected to large wind loads. Wind loads have caused numerous fatigue problems in sign, signal, and luminaire support structures [32], transmission towers, and chimneys.

Although cracks can form in structures cycled in compression, they arrest and are not structurally significant. Therefore, only members or connections for which the stress cycle is at least partially in tension need to be assessed. If a fatigue crack forms in one element of a bolted or riveted built-up structural member, the crack cannot propagate directly into neighboring elements. Usually, a riveted member will not fail until a second crack forms in another element. Therefore, riveted built-up structural members are inherently redundant. Once a fatigue crack forms, it can propagate directly into all elements of a continuous welded member and cause failure at service loads. The lack of

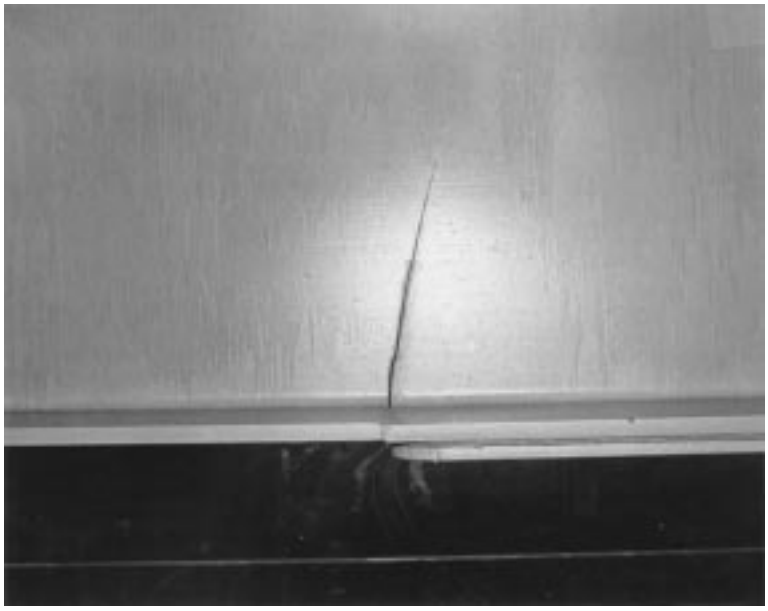

FIGURE 24.3: Fatigue crack originating from the weld toe of a coverplate end detail in one of the Yellow Mill Pond structures.

inherent redundancy in welded members is one reason that fatigue and fracture changed from a nuisance to a significant structural integrity problem as welding became widespread in the 1940s. Welded structures are not inferior to bolted or riveted structures; they just require more attention to design, detailing, and quality.

In structures such as bridges and ships, the ratio of the fatigue-design load to the strength-design loads is large enough that fatigue may control the design of much of the structure. In long-span bridges, the load on much of the superstructure is dominated by the dead load, with the fluctuating live load relatively small. These members will not be sensitive to fatigue. However, the deck, stringers, and floorbeams of bridges are subjected to primarily live load and therefore may be controlled by fatigue.

In structures controlled by fatigue, fracture is almost always preceded by fatigue cracking; therefore, the primary emphasis should be on preventing fatigue. Usually, the steel and filler metal have minimum specified toughness values (such as a Charpy V-Notch [CVN] test requirement). In this case, the cracks can grow to be quite long before fracture occurs. Fatigue cracks grow at an exponentially increasing rate; therefore, most of the life transpires while the crack is very small. Additional fracture toughness, greater than the minimum specified values, will allow the crack to grow to a larger size before sudden fracture occurs. However, the crack is growing so rapidly at the end of life that the additional toughness may increase the life only insignificantly.

However, fracture is possible for buildings that are not subjected to cyclic loading. Several large tension chords of long-span trusses fractured while under construction in the 1980s. The tension chords consisted of welded jumbo shapes, i.e., shapes in groups 4 and 5, as shown in Figure 24.4 [22]. These jumbo shapes are normally used for columns, where they are not subjected to tensile stress. These sections often have low fracture toughness, particularly in the core region of the web and flange junction. The low toughness has been attributed to the relatively low rolling deformation and slow cooling in these thick shapes. The low toughness is of little consequence if the section is used as a column and remains in compression. The fractures of jumbo tension chords occurred at welded

FIGURE 24.4: (a) View of jumbo section used as tension chord in a roof truss and (b) closeup view of fracture in web originating from weld access holes at welded splice.

splices at groove welds or at flame-cut edges of cope holes, as shown in Figure 24.4. In both cases the cracks formed at cope holes in the hard layer formed from thermal cutting. These cracks propagated in the core region of these jumbo sections, which has very low toughness. As a consequence of these brittle fractures, AISC (American Institute of Steel Construction) specifications now have a supplemental CVN notch toughness requirement for shapes in groups 4 and 5 and (for the same reasons) plates greater than 51 mm thick, when these are welded and subject to primary tensile stress from axial load or bending. Poorly prepared cope holes have resulted in cracks and fractures in lighter shapes as well.

The detailing rules that are used to prevent fatigue are intended to avoid notches and other stress concentrations. These detailing rules are useful for the avoidance of brittle fracture as well as fatigue. For example, the detailing rules in AASHTO (American Association of State Highway Transportation Officials) bridge design specifications would not permit a backing bar to be left in place because of the unfused notch perpendicular to the tensile stress in the flange. Along with low-toughness weld metal, this type of backing bar notch was a significant factor in the brittle fracture of WSMF connections in the Northridge earthquake [33, 53, 55]. Figure 24.5 shows a cross-section of a beam-flange-to-column weld from a building that experienced such a fracture. It is clear that the crack emanated from the notch created by the backing bar.

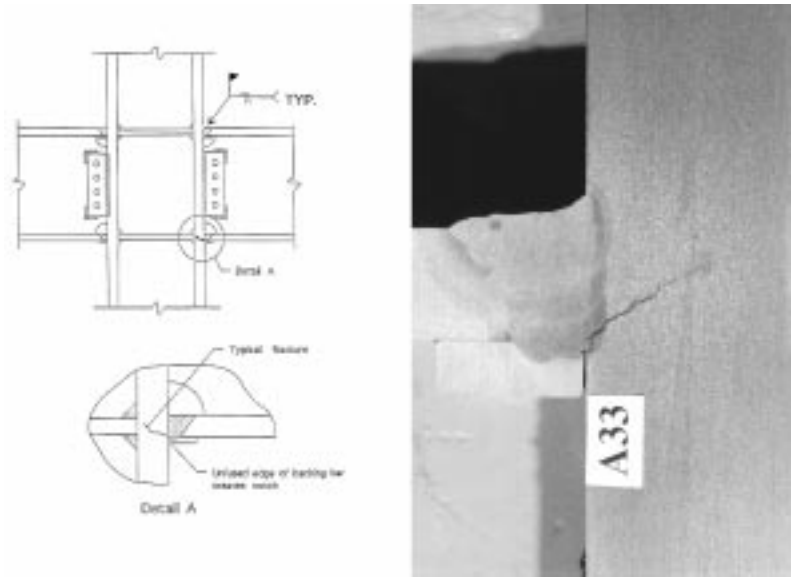

FIGURE 24.5: Welded steel moment frame (WSMF) connection showing (a) location of typical fractures and (b) typical crack, which originated at the backing bar notch and propagated into the column flange.

Detailing rules similar to the AASHTO detailing rules are included in American Welding Society (AWS) D1.1 *Structural Welding Code—Steel* for dynamically loaded structures. Dynamically loaded has been interpreted to mean fatigue loaded. Unfortunately, most seismically loaded building frames have not been required to be detailed in accordance with these rules. Even though it is not required, it might be prudent in seismic design to follow the AWS D1.1 detailing rules for all dynamically loaded structures.

Design for fracture resistance in the event of an extreme load is more qualitative than fatigue design, and usually does not involve specific loads. Details are selected to maximize the strength and ductility without increasing the basic section sizes required to satisfy strength requirements. The objective is to get the yielding to spread across the cross-section and develop the reserve capacity of the structural system without allowing premature failure of an individual component to precipitate total failure of the structure. The process of design for fracture resistance involves (1) predicting conceivable failure modes due to extreme loading, then (2) correctly selecting materials for and detailing the "critical" members and connections involved in each failure mode to achieve maximum ductility. Critical members and connections are those that are required to yield, elongate, or form a plastic hinge before the ultimate strength can be achieved for these conceived failure modes. Usually, the cost to upgrade a design meeting strength criteria to also be resistant to fatigue and fracture is very reasonable. The cost may increase due to (1) details that are more expensive to fabricate, (2) more expensive welding procedures, and (3) more expensive materials.

Quantitative means for assessing fracture are presented. Because of several factors, there is at best only about ± 30% accuracy in these fracture predictions, however. These factors include (1) variability of material properties; (2) changes in apparent toughness values with changes in test specimen size and geometry; (3) differences in toughness and strength of the weld zone; (4) complex residual stresses; (5) high gradients of stress in the vicinity of the crack due to stress concentrations; and (6) the behavior of cracks in complex structures of welded intersecting plates.

24.2 Design and Evaluation of Structures for Fatigue

Testing on full-scale welded members has indicated that the primary effect of constant amplitude loading can be accounted for in the live-load stress range [15, 20, 21, 34]; that is, the mean stress is not significant. The reason that the dead load has little effect on the lower bound of the results is that, locally, there are very high residual stresses. In details that are not welded, such as anchor bolts, there is a strong mean stress effect [54]. A worst-case conservative assumption (i.e., a high-tensile mean stress) is made in the testing and design of these nonwelded details.

The strength and type of steel have only a negligible effect on the fatigue resistance expected for a particular detail. The welding process also does not typically have an effect on the fatigue resistance. The independence of the fatigue resistance from the type of steel greatly simplifies the development of design rules for fatigue since it eliminates the need to generate data for every type of steel.

The established approach for fatigue design and assessment of metal structures is based on the S-N curve. Typically, small-scale specimen tests will result in longer apparent fatigue lives. Therefore, the S-N curve must be based on tests of full-size structural components such as girders. The reasons for these scale effects are discussed in Section 24.2.2. When information about a specific crack is available, a fracture mechanics crack growth rate analysis should be used to calculate remaining life [9, 10]. However, in the design stage, without specific initial crack size data, the fracture mechanics approach is not any more accurate than the S-N curve approach [35]. Therefore, the fracture mechanics crack growth analysis will not be discussed further.

Welded and bolted details for bridges and buildings are designed based on the nominal stress range rather than the local "concentrated" stress at the weld detail. The nominal stress is usually obtained from standard design equations for bending and axial stress and does not include the effect of stress concentrations of welds and attachments. Usually, the nominal stress in the members can be easily calculated without excessive error. However, the proper definition of the nominal stresses may become a problem in regions of high stress gradients.

The lower-bound S-N curves for steel in the AASHTO, AISC, AWS, and the American Railway Engineers Association (AREA) provisions are shown in Figure 24.6. These S-N curves are based on a lower bound with a 97.5% survival limit. S-N curves are presented for seven categories (A through

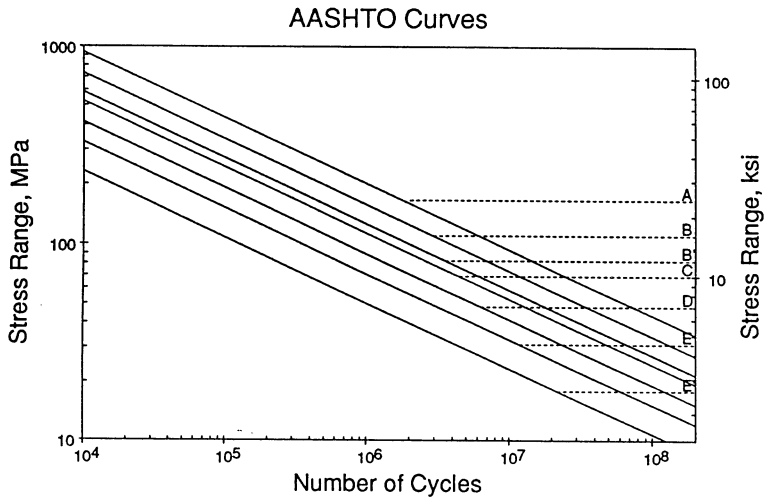

FIGURE 24.6: The AASHTO/AISC S-N curves. Dashed lines are the constant-amplitude fatigue limits and indicate the detail category.

E′) of weld details. The effect of the welds and other stress concentrations is reflected in the ordinate of the S-N curves for the various detail categories. The slope of the regression line fit to the test data for welded details is typically in the range 2.9 to 3.1 [34]. Therefore, in the AISC and AASHTO codes as well as in Eurocode 3 [18], the slopes have been standardized at 3.0.

Figure 24.6 shows the constant-amplitude fatigue limits (CAFLs) for each category as horizontal dashed lines. The CAFLs in Figure 24.6 were determined from the full-scale test data. When constant-amplitude tests are performed at stress ranges below the CAFL, noticeable cracking does not occur. Note that for all but category A, the fatigue limits occur at numbers of cycles much greater than two million, and therefore the CAFL should not be confused with the fatigue strength. Fatigue strength is a term representing the nominal stress range corresponding to the lower-bound S-N curve at a particular number of cycles, usually two million cycles. Most structures experience what is known as long-life variable-amplitude loading, i.e., very large numbers of random-amplitude cycles greater than the number of cycles associated with the CAFL. For example, a structure loaded continuously at an average rate of three times per minute (0.05 Hz) would accumulate 10 million cycles in only 6 years. The CAFL is the only important property of the S-N curve for long-life variable-amplitude loading, as discussed further in Section 24.2.4.

Similar S-N curves have been proposed by the Aluminum Association for welded aluminum structures. Table 24.1 summarizes the CAFLs for steel and aluminum for categories A through E'. The design procedures are based on associating weld details with specific categories. For both steel and aluminum, the separation of details into categories is approximately the same. Since fatigue is typically only a serviceability problem, fatigue design is carried out using service loads.

The nominal stress approach is simple and sufficiently accurate, and therefore is preferred when applicable. However, for details not covered by the standard categories, or for details in the presence of secondary stresses or high-stress gradients, the "hot-spot" stress range approach may be the only alternative. The hot-spot stress range is the stress range in a plate normal to the weld axis at some small distance from the weld toe. The hot-spot stress may be determined by strain gage measurement, finite element analysis, or empirical formulas. Unfortunately, methods and locations for measuring or calculating hot-spot stress as well as the associated S-N curve vary depending on which code or recommendation is followed [56].

TABLE 24.1 Constant-Amplitude Fatigue Limits for AASHTO and Aluminum Association S-N Curves

Detail category	CAFL for steel (MPa)	CAFL for aluminum (MPa)
A	165	70
B	110	41
B′	83	32
C	69	28
D	48	17
E	31	13
E′	18	7

In U.S. practice (i.e., the hot-spot method that has been used with the American Petroleum Institute's API RP-2A and AWS D1.1) the hot-spot stress is determined with a strain gage located nominally 5mm from the weld toe [16]. Actually, the 5-mm distance was not specifically selected. Rather, this distance was just the closest to the weld toe that a 3-mm strain gage could be placed. This definition of hot-spot stress originated from early experimental work on pressure vessels and tubular joints and has been the working definition of hot-spot stress in the U.S. offshore industry [40]. This approach is also used for other welded tubular joints and for details in ships and other marine structures.

The S-N curve used with the hot-spot stress approach is essentially the same as the nominal stress S-N curve (category C) for a transverse butt or fillet weld in a nominal membrane stress field (i.e., a stress field without any global stress concentration). The geometrical stress concentration and discontinuities associated with the local weld toe geometry are built into the S-N curve, while the global stress concentration is included in the hot-spot stress range.

24.2.1 Classification of Structural Details for Fatigue

It is standard practice in fatigue design of welded structures to separate the weld details into categories having similar fatigue resistance in terms of the nominal stress. Most common details can be idealized as analogous to one of the drawings in the specifications. The categories in Figure 24.6 range from A to E′ in order of decreasing fatigue strength. There is an eighth category, F, in the specifications, which applies to fillet welds loaded in shear. However, there have been very few if any failures related to shear, and the stress ranges are typically very low such that fatigue rarely would control the design. Therefore, the shear stress category F will not be discussed further.

In fact there have been very few if any failures attributed to details that have a fatigue strength greater than category C. Most structures have many more severe details, and these will generally govern the fatigue design. Therefore, unless all connections in highly stressed elements of the structure are high-strength bolted connections rather than welded, it is usually a waste of time to check category C and better details. Therefore, only category C and more severe details will be discussed in this section.

Severely corroded members should be evaluated to determine the stress range with respect to the reduced thickness and loss of section. Corrosion notches and pits may lead to fatigue cracks and should be specially evaluated. Otherwise severely corroded members may be treated as category E [44].

In addition to being used by AISC and AASHTO specifications, the S-N curves in Figure 24.6 and detail categories are essentially the same as those adopted by the AREA and AWS *Structural Welding Code* D1.1. The AASHTO/AISC S-N curves are also the same as 7 of the 11 S-N curves in the Eurocode 3. The British Standard (BS) 7608 has slightly different S-N curves, but these can be correlated to the nearest AISC S-N curve for comparison.

The following is a brief simplified overview of the categorization of fatigue details. In all cases, the applicable specifications should also be checked. Several reports have been published that show a large number of illustrations of details and their categories in addition to those in AISC and AASHTO

specifications [14, 57]. Also, the Eurocode 3 and the BS 7608 have more detailed illustrations for their categorization than does the AISC or AASHTO specifications. Maddox [38] discusses categorization of many details in accordance with BS 7608, from which roughly equivalent AISC categories can be inferred.

In most cases, the fatigue strength recommended in these European standards is similar to the fatigue strength in the AISC and AASHTO specifications. However, there are several cases where the fatigue strength is significantly different; usually the European specifications are more conservative. Some of these cases are discussed in the following, as well as the fatigue strength for details that are not found in the specifications.

Mechanically Fastened Joints

Small holes are considered category D details. Therefore, rivetted and mechanically fastened joints (other than high-strength bolted joints) loaded in shear are evaluated as category D in terms of the net-section nominal stress. Pin plates and eyebars are designed as category E details in terms of the stress on the net section. In the AISC specifications, bolted joints loaded in direct tension are evaluated in terms of the maximum unfactored tensile load, including any prying load. Typically, these provisions are applied to hanger-type or bolted flange connections where the bolts are tensioned against the plies. If the number of cycles exceeds 20,000, the allowable load is reduced relative to the allowable load for static loading. Prying is very detrimental to fatigue, so if the number of cycles exceeds 20,000, it is advisable to minimize prying forces.

When bolts are tensioned against the plies, the total fluctuating load is resisted by the whole area of the precompressed plies, so that the bolts are subjected to only a fraction of the total load [37]. The analysis to determine this fraction is difficult, and this is one reason that the bolts are designed in terms of the maximum load rather than a stress range in the AISC specifications. In BS 7608, a slightly different approach is used for bolts in tension that achieves approximately the same result as the AISC specification for high-strength bolts. The stress range, on the tensile stress area of the bolt, is taken as 20% of the total applied load, regardless of the fluctuating part of the total load. The S-N curve for bolts is proportional to F_u, so that for high-strength bolts the result is an S-N curve between category E and E′ for cycles less than two million. The tensile stress area, A_t, is given by

$$A_t = \frac{\pi}{4}\left(d_b - \frac{0.9743}{n}\right)^2 \tag{24.1}$$

where

d_b = the nominal diameter (the body or shank diameter)

n = threads per inch

(Note that the constant would be different if SI units were used.)

In the Eurocode 3, the fatigue strength of bolts is given in terms of the actual stress range in the bolts, although it is not clear how to calculate this for pretensioned connections. The recommended fatigue strength is given in terms of the tensile stress area of the bolt and does not depend on tensile strength. The design S-N curve from Eurocode 3 is about the same as category E′, which is consistent with BS 7608 for high-strength bolts.

Anchor bolts in concrete cannot be adequately pretensioned and therefore do not behave like hanger-type or bolted flange connections. At best they are pretensioned between nuts on either side of the column base plate and the part below the bottom nut is still exposed to the full load range. Some additional test data was recently generated at the ATLSS Center at Lehigh University [54] for grade 55 and grade 105 anchor bolts. When combined with the existing data [27], the data show that the fatigue strength for anchor bolts is slightly greater than category E′ in terms of the stress range on the tensile stress area of the bolt. Some of the bolts were tested with an intentional misalignment

of 1:40, and these had only slightly lower fatigue strength than the aligned bolts, bringing the lower bound of the data closer to the category E′ S-N curve.

The ATLSS data show the CAFL for all anchor bolts is slightly greater than the category D CAFL (48 MPa). The ATLSS data and Karl Frank's data show that proper tightening between the double nuts had a slight beneficial effect on the CAFL, but not enough to increase it by one category. In summary, for all types of bolts, if the actual stress range on the tensile stress area can be determined, it is recommended that (1) for finite life, the category E′ S-N curve be used, and (2) for infinite life, the CAFL equivalent to that for category D be used (48 MPa).

Welded Joints

Welded joints are considered longitudinal if the axis of the weld is parallel to the primary stress range. Continuous longitudinal welds are category B or B′ details. However, the termination of longitudinal fillet welds is more severe (category E). (The termination of full-penetration groove longitudinal welds requires a ground transition radius but gives a greater fatigue strength, depending on the radius.) If longitudinal welds must be terminated, it is better to terminate at a location where the stress ranges are less severe.

Category C includes transverse full-penetration groove welds (butt joints) subjected to nondestructive evaluation (NDE). Experiments conducted at Lehigh University showed that groove welds containing large internal discontinuities that were not screened out by NDE had a fatigue strength comparable to category E. The BS 7608 and the British Standards Institute published document PD 6493 [12] have reduced fatigue strength curves for groove welds with defects that are generally in agreement with these experimental data. Transverse groove welds with a permanent backing bar are reduced to category D [38]. One-sided welds with melt through (without backing bars) are also classified as category D.

Cope holes for weld access and to avoid intersecting welds, with edges conforming to the ANSI (American National Standards Institute) smoothness of 1000, may be considered a category D detail. Poorly executed cope holes must be treated as a category E detail. In some cases small cracks have occurred from the thermal-cut edges if martensite is developed. In those cases, crack extension will occur at lower stress ranges. Testing performed at ATLSS as well as at TNO in the Netherlands [17] has shown that the cope hole has lower fatigue strength than overlapping welds, which are less expensive but have traditionally been avoided because of the discontinuity at the overlap.

There have been many fatigue-cracking problems in structures at miscellaneous and seemingly unimportant attachments to the structure for such things as racks and hand rails. Attachments are a "hard spot" on the strength member that create a stress concentration at the weld. Often, it is not realized that such secondary members become part of the girder, i.e., that these secondary members stretch with the girder and therefore are subject to large stress ranges. Consequently, problems have occurred with fatigue of such secondary members.

Attachments normal to flanges or plates that do not carry significant load are rated category C if less than 51 mm long in the direction of the primary stress range, D if between 51 and 101 mm long, and E if greater than 101 mm long. (The 101-mm limit may be smaller for plates thinner than 9 mm.) If there is not at least 10 mm edge distance, then category E applies for an attachment of any length. The category E′, slightly worse than category E, applies if the attachment plates or the flanges exceed 25 mm in thickness. Transverse stiffeners are treated as short attachments (category C). Note that the attachment to the round tube in the crane boom in Figure 24.1, the transverse attachment in the vehicle frame in Figure 24.2, and the coverplate end detail in Figure 24.3 are all category E and E′ attachments.

The cruciform joint where the load-carrying member is discontinuous is considered a category C detail because it is assumed that the plate transverse to the load-carrying member does not have any stress range. A special reduction factor for the fatigue strength is provided when the load-carrying

plate exceeds 13 mm in thickness. This factor accounts for the possible crack initiation from the unfused area at the root of the fillet welds (as opposed to the typical crack initiation at the weld toe for thinner plates) [26]. An example of cracking through the fillet weld throat of an attachment plate is shown in Figure 24.7.

FIGURE 24.7: Cracking through the throat of fillet welds on an attachment plate.

Transverse stiffeners that are used for cross-bracing or diaphragms are also treated as category C details with respect to the stress in the main member. In most cases, the stress range in the stiffener from the diaphragm loads is not considered because these loads are typically unpredictable. In any case, the stiffener must be attached to the flanges, so even if the transverse loads were significant, most of the load would be transferred in shear to the flanges. (The web has very little out-of-plane stiffness.) In theory, the shear stress range in the fillet welds to the flanges should be checked, but shear stress ranges rarely govern design.

In most other types of load-carrying attachments, there is interaction between the stress range in the transverse load-carrying attachment and the stress range in the main member. In practice, each of these stress ranges is checked separately. The attachment is evaluated with respect to the stress range in the main member and then it is separately evaluated with respect to the transverse stress range. The combined multiaxial effect of the two stress ranges is taken into account by a decrease in the fatigue strength; that is, most load-carrying attachments are considered category E details. Multiaxial effects are discussed in greater detail in Section 24.2.3.

If the fillet or groove weld ends of a longitudinal attachment (load bearing or not) are ground smooth to a transition radius greater than 50 mm, the attachment can be considered category D (load bearing or not). If the transition radius of a groove-welded longitudinal attachment is increased to greater than 152 mm (with the groove-weld ends ground smooth), the detail (load bearing or not) can be considered category C.

Misalignment is a primary factor in susceptibility to cracking. The misalignment causes eccentric loading, local bending, and stress concentration. If the ends of a member with a misaligned connection are essentially fixed, the stress concentration factor (SCF) associated with misalignment is

$$\text{SCF} = 1.0 + 3e/t \tag{24.2}$$

where e is the eccentricity and t is the smaller of the thicknesses of two opposing loaded members. The nominal stress times the SCF should then be compared to the appropriate category. Generally, such misalignment should be avoided at fatigue critical locations. Equation 24.2 can also be used where e is the distance that the weld is displaced out of plane due to angular distortion. In either case, if the ends are pinned, the SCF is twice as large. A thorough guide to the SCF for various types of misalignment and distortion, including plates of unequal thickness, can be found in the British Standards Institute published document PD 6493 [12].

Reinforced and Prestressed Concrete and Bridge Stay Cables

Concrete structures are typically less sensitive to fatigue than welded steel and aluminum structures. However, fatigue may govern the design when impact loading is involved, such as for pavement, bridge decks, and rail ties. Also, as the age of concrete girders in service increases, and as the applied stress ranges increase with increasing strength of concrete, the concern for fatigue in concrete structural members has also increased.

According to ACI (American Concrete Institute) Committee Report 215R-74 in the *Manual of Standard Practice* [2], the fatigue strength of plain concrete at 10 million cycles is approximately 55% of the ultimate strength. However, even if failure does not occur, repeated loading may contribute to premature cracking of the concrete, such as inclined cracking in prestressed beams. This cracking can then lead to localized corrosion and fatigue of the reinforcement [30].

The fatigue strength of straight, unwelded reinforcing bars and prestressing strand can be described (in terms of the categories for steel details) with the category B S-N curve. The lowest stress range that has been known to cause a fatigue crack in a straight reinforcing bar is 145 MPa, which occurred after more than a million cycles. As expected, based on the results for steel details, minimum stress and yield strength had minimal effect on the fatigue strength of reinforcing bars. Bar size, geometry, and deformations also had minimal effect. ACI Committee 215 [2] suggested that members be designed to limit the stress range in the reinforcing bar to 138 MPa for high levels of minimum stress (possibly increasing to 161 MPa for less minimum stress). Fatigue tests show that previously bent bars had only about half the fatigue strength of straight bars, and failures have occurred down to 113 MPa [47]. Committee 215 recommends that half of the stress range for straight bars be used (i.e., 69 MPa) for the worst-case minimum stress. Equating this recommendation to the S-N curves for steel details, bent reinforcement may be treated as a category D detail.

Provided the quality is good, butt welds in straight reinforcing bars do not significantly lower the fatigue strength. However, tack welds reduce the fatigue strength of straight bars about 33%, with failures occurring as low as 138 MPa. Fatigue failures have been reported in welded wire fabric and bar mats [51].

If prestressed members are designed with sufficient precompression that the section remains uncracked, there is not likely to be any problem with fatigue. This is because the entire section is resisting the load ranges and the stress range in the prestessing strand is minimal. Similarly, for unbonded prestressed members, the stress ranges will be very small. Although the fatigue strength of prestressing strand in air is about equal to category B, when the anchorages are tested as well, the fatigue strength of the system is as low as half the fatigue strength of the wire alone (i.e., about category E). However, there is reason to be concerned for bonded prestressing at cracked sections because the stress range increases locally. The concern for cracked sections is even greater if corrosion is involved. The pitting from corrosive attack can dramatically lower the fatigue strength of reinforcement [30].

The above data were generated in tests of the prestressing systems in air. When actual beams are tested, the situation is very complex, but it is clear that much lower fatigue strength can be obtained [45, 48]. Committee 215 has recommended the following for prestressed beams:

1. The stress range in prestressed reinforcement, determined from an analysis considering the section to be cracked, shall not exceed 6% of the tensile strength of the reinforcement.

(*Note*: This is approximately equivalent to category C.)

2. Without specific experimental data, the fatigue strength of unbonded reinforcement and their anchorages shall be taken as half of the fatigue strength of the prestressing steel. (*Note*: This is approximately equivalent to Category E.) Lesser values shall be used at anchorages with multiple elements.

The Post-Tensioning Institute (PTI) has issued "Recommendations for Stay Cable Design and Testing". The PTI recommends that uncoupled bar stay cables are category B details, while coupled (glued) bar stay cables are category D. The fatigue strengths of stay cables are verified through fatigue testing. Two types of tests are performed: (1) fatigue testing of the strand and (2) testing of relatively short lengths of the assembled cable with anchorages. The recommended test of the system is two million cycles at a stress range (158 MPa) that is 35 MPa greater than the fatigue allowable for category B at two million cycles. This test should pass with less than 2% wire breaks. A subsequent proof test must achieve 95% of the actual ultimate tensile strength of the tendons.

24.2.2 Scale Effects in Fatigue

As previously mentioned, fatigue tests on small-scale specimens will give higher apparent fatigue strength and are therefore unconservative [39, 41, 46]. There are several possible reasons for the observed scale effects. First, there is a well-known thickness effect in fatigue. This thickness effect is reflected in many places in AASHTO and AISC specifications where the fatigue strength is reduced for details with plate thickness greater than 20 or 25 mm in certain cases. For example, when coverplates exceed 25 mm in thickness or are wider than the flange, category E′ applies rather than category E. However, there may be cases where the coverplate is both wider than the flange and thicker than 25 mm. The fatigue strength in this case may be even less than category E′. One such case is shown in Figure 24.8, which is a wind-bracing gusset attached to the bottom of a floorbeam flange. The fatigue crack began at the termination of the fillet weld (along the top weld toe) where the plates overlap gusset laps.

In BS 7608, the fatigue strength of many details are keyed to plates with thickness 16 mm and less. For plates exceeding 16 mm, an equation is given that reduces the fatigue strength for thicker plates. A similar equation is used in Eurocode 3 for plates greater than 25 mm thick. These equations produce reductions in fatigue strength proportional to the 1/4 power of the ratio of the thickness to the base thickness (i.e., 16 or 25 mm).

Another effect is that the applied stress range may be different in small-scale specimens. For example, the stress concentration associated with welded attachments varies with the length of the attachment in the direction of the stresses. Also, in large-scale specimens, even though the nominal stress state is uniaxial or bending, unique local multiaxial stress states may develop naturally in complex details from random stress concentrations (e.g., poor workmanship and weld shape) and eccentricities (e.g., asymmetry of the design, tolerances, misalignment, distortion from welding). These complex natural stress states may be difficult to simulate in small-scale specimens and are difficult if not impossible to simulate analytically.

The state of residual stress from welding may be significantly different for small specimens due to the lack of constraint. Even if the specimens are cut from large-scale members, the residual stress will be altered. Finally, the volume of weld metal in full-scale members is sufficient to contain a structurally relevant representative sample of discontinuities (e.g., microcracks, pores, slag inclusions, hydrogen cracks, tack welds, and other notches).

FIGURE 24.8: Fatigue crack originating from the upper weld toe of a fillet weld where the fillet weld terminates near the overlap of thick plates.

24.2.3 Distortion and Multiaxial Loading Effects in Fatigue

In the AASHTO/AISC fatigue design provisions, the loading is assumed to be simple uniaxial loading. However, the loading may often be more complex than is commonly assumed in design. For example, fatigue design is based on the primary tension and bending stress ranges. Torsion, racking, transverse bending, and membrane action in plating are considered secondary loads and are typically not considered in fatigue analysis.

However, it is clear from the type of cracks that occur in bridges that a significant proportion of the cracking is due to distortion resulting from such secondary loading [24]. The solution to the problem of fatigue cracking due to secondary loading usually relies on the qualitative art of good detailing. Often, the best solution to distortion cracking problems may be to stiffen the structure. Typically, the

better connections are more rigid. For example, transverse bracing and floorbeam attachment plates on welded girders should be welded directly to both flanges as well as the web. Numerous fatigue cracks have occurred due to distortion in the "web gap", i.e., the narrow gap between the stiffener and the flange. Figure 24.9 shows an example of a longitudinal crack formed along the longitudinal fillet weld that originated in the web gap (between the top of the stiffener and the flange) when such attachment plates are not welded to the flange. There has been a tendency to avoid welding to the tension flange due to an unfounded concern about brittle fracture.

FIGURE 24.9: Typical distortion-induced cracking in the web gap of an attachment plate.

In some cases a better solution is to allow the distortion to take place over a greater area so that lower stresses are created; that is, the detail should be made more flexible. For example, if a transverse stiffener is not welded to a flange, it is important to ensure that the gap between the flange and the end of the stiffener is sufficiently large, between four and six times the thickness of the web [23]. Another example where the best details are more flexible is connection angles for simply supported beams. Despite our assumptions, such simple connections transmit up to 40% of the theoretical fixed-end moment, even though they are designed to transmit only shear forces. For a given load, the moment in the connection decreases significantly as the rotational stiffness of the connection decreases. The increased flexibility of connection angles allows the limited amount of end rotation to take place with reduced bending stresses. A criterion has been developed for the design of these angles to provide sufficient flexibility [58]. The criterion states that the angle thickness (t) must be

$$t < 12\left(g^2/L\right) \tag{24.3}$$

where g is the gage in inches and L is the span length in inches. For example, for connection angles with a gage of 76 mm and a beam span of 7 m, the angle thickness should be just less than 10 mm. To solve a connection-angle cracking problem in service, the topmost rivet or bolt may be removed and replaced with a loose bolt to ensure the shear capacity. For loose bolts, steps are required to ensure that the nuts do not back off.

Significant stresses from secondary loading are often in a different direction than the primary stresses. Fortunately, experience with multiaxial loading experiments on large-scale welded structural

details indicates the loading perpendicular to the local notch or the weld toe dominates the fatigue life. The cyclic stress in the other direction has no effect if the stress range is below 83 MPa and only a small influence above 83 MPa [16, 24].

The recommended approach for multiaxial loads is

1. Decide which loading (primary or secondary) dominates the fatigue cracking problem (typically the loading perpendicular to the weld axis or perpendicular to where cracks have previously occurred in similar details).
2. Perform the fatigue analysis using the stress range in this direction (i.e., ignore the stresses in the orthogonal directions).

24.2.4 The Effective Stress Range for Variable-Amplitude Loading

An actual service load history is likely to consist of cycles with a variety of different load ranges, i.e., variable-amplitude loading [25]. However, the fatigue design provisions are based on constant-amplitude loading and do not give any guidance for variable-amplitude loading. A procedure is shown below to convert variable stress ranges to an equivalent constant-amplitude stress range with the same number of cycles. This procedure is based on the damage summation rule jointly credited to Palmgren and Miner (referred to as Miner's rule) [42]. If the slope of the S-N curve is equal to 3, then the relative damage of stress ranges is proportional to the cube of the stress range. Therefore, the effective stress range is equal to the cube root of the mean cube of the stress ranges, i.e.,

$$S_{\text{effective}} = \left[(n_i / N_{\text{total}})\, S_i^3 \right]^{1/3} \tag{24.4}$$

The LRFD (load and resistance factor design) version of the AASHTO specification implies such an effective stress range using the straight line extension of the constant-amplitude curve. This is essentially the approach for variable-amplitude loading in BS 7608. Eurocode 3 also uses the effective stress range concept.

Research on such high-cycle variable-amplitude fatigue has shown that if all but 0.01% of the stress ranges are below the CAFLs, fatigue cracking does not occur [25]. The simplified fatigue-design procedure in the *AASHTO LRFD Bridge Design Specifications* [1] for structures with very large numbers of cycles is based on this observation. The objective of the AASHTO fatigue-design procedure is to ensure that the stress ranges at critical details due to a fatigue limit state load range are less than the CAFL for the particular details. The fatigue limit state load range is defined as having a probability of exceedence over the lifetime of the structure of 0.01%. A structure with millions of cycles is likely to see load ranges with this magnitude or greater hundreds of times; therefore, the fatigue limit state load range is not as large as the extreme loads used to check ultimate strength.

24.2.5 Low-Cycle Fatigue Due to Seismic Loading

Steel-braced frames and moment-resisting frames are expected to withstand cyclic plastic deformation without cracking in a large earthquake. If brittle fracture of these moment frame connections is suppressed, the connections can be cyclically deformed into the plastic range and will eventually fail by tearing at a location of strain concentration. This failure mode can be characterized as low-cycle fatigue. Low-cycle fatigue has been studied for pressure vessels and some other types of mechanical engineering structures. Since low-cycle fatigue is an inelastic phenomenon, the strain range is the key parameter rather than the stress range. However, at this time very little is understood about low-cycle fatigue in structures. For example, it is a very difficult task just to predict accurately the local strain range at a location of cyclic buckling.

Research performed to date indicates the feasibility of predicting curves for low-cycle fatigue from strain range vs. number of cycles in a manner analogous to high-cycle fatigue design using stress-range-based S-N curves. For example, low-cycle fatigue experiments were performed on specimens that would buckle as well as compact specimens that would not buckle but rather would fail from cracking at the welds [36]. These tests showed that the number of cycles to failure by low-cycle fatigue of welded connections could be predicted by the local strain range in a power law that is analogous to the power law (with stress range) represented by an S-N curve. They also showed that Miner's rule could be used to predict the number of variable-amplitude cycles to failure based on constant-amplitude test data.

More recently, Castiglioni [8, 13] has conducted similar experiments and plotted the results in terms of a fictitious elastic stress range that is equal to the strain range times the modulus of elasticity. In this manner he has shown that the low-cycle fatigue data plot along the same S-N curves from the Eurocode (similar to the AASHTO S-N curves) that are normally used for high-cycle fatigue. Castiglioni has equated the slenderness of the flanges with different fatigue categories, in effect treating the propensity for buckling like a "notch".

It can be hypothesized from these preliminary data that the same model used for high-cycle fatigue design, i.e., the S-N curves (converted to strain), can be used to predict fatigue behavior in the very-low-cycle regime characteristic of earthquake loading. Such a model could be very useful in seismic design of welded and bolted steel connections. Just by inspection, alternative details for a connection can be ranked in accord with their expected fatigue strength, i.e., the expected strain range that would cause cracking after a certain minimum number of cycles. After some limited verification through very-low-cycle inelastic experiments, these comparisons could rely on the existing knowledge base for the relative fatigue strength of various details in high-cycle fatigue.

The detailing rules that are used to prevent high-cycle fatigue are intended to avoid notches and other stress concentrations. These detailing rules could also be useful for preventing brittle fracture and premature low-cycle fatigue cracking. The relative fatigue strength is given by the detail category and the corresponding S-N curve.

24.3 Evaluation of Structural Details for Fracture

Unlike fatigue, fracture behavior depends strongly on the type and strength level of the steel or filler metal. In general, fracture toughness has been found to decrease with increasing yield strength of a material, suggesting an inverse relationship between the two properties. In practice, however, fracture toughness is more complex than implied by this simple relationship since steels with similar strength levels can have widely varying levels of fracture toughness.

Steel exhibits a transition from brittle to ductile fracture behavior as the temperature increases. For example, Figure 24.10 shows a plot of the energy required to fracture CVN impact test specimens of A588 structural steel at various temperatures. These results are typical for ordinary hot-rolled structural steel. The transition phenomena shown in Figure 24.10 is a result of changes in the underlying microstructural fracture mode. There are really at least three distinct types of fracture with distinctly different behavior.

1. *Brittle fracture* is associated with cleavage, which is transgranular fracture on select crystallographic planes on a microscopic scale. This type of fracture occurs at the lower end of the temperature range, although the brittle behavior can persist up to the boiling point of water in some low-toughness materials. This part of the temperature range is called the lower shelf because the minimum toughness is fairly constant up to the transition temperature. Brittle fracture is sometimes called elastic fracture because the plasticity that occurs is negligible and consequently the energy absorbed in the fracture process is also negligible.

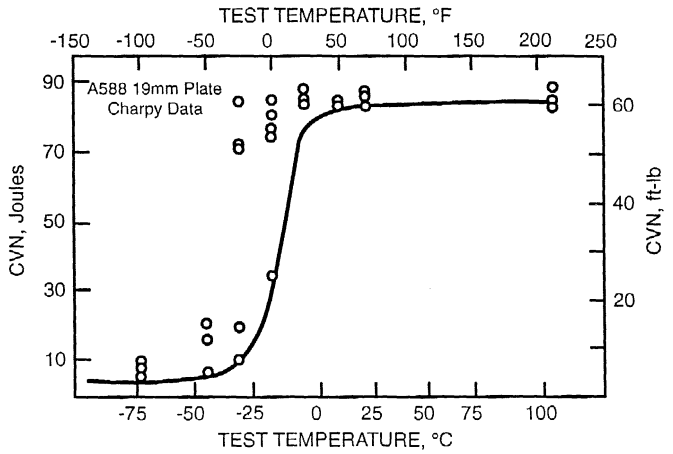

FIGURE 24.10: Charpy energy transition curve for A588 grade 50 (350-MPa yield strength) structural steel.

2. *Transition-range fracture* occurs at temperatures between the lower shelf and the upper shelf and is associated with a mixture of cleavage and fibrous fracture on a microstructural scale. Because of the mixture of micromechanisms, transition-range fracture is characterized by extremely large variability. Fracture in the transition region is sometimes referred to as elastic-plastic fracture because the plasticity is limited in extent but has a significant impact on the toughness.
3. *Ductile fracture* is associated with a process of void initiation, growth, and coalescence on a microstructural scale, a process requiring substantial energy, and occurs at the higher end of the temperature range. This part of the temperature range is referred to as the upper shelf because the toughness levels off and is essentially constant for higher temperatures. Ductile fracture is sometimes called fully plastic fracture because there is substantial plasticity across most of the remaining cross-section ahead of a crack. Ductile fracture is also called fibrous fracture due to the fibrous appearance of the fracture surface, or shear fracture due to the usually large slanted shear lips on the fracture surface.

Ordinary structural steel such as A36 or A572 is typically only hot rolled. To achieve very high-toughness, steels must be controlled rolled, i.e., rolled at lower temperatures, or must receive some auxiliary heat treatment such as normalization. In contrast to the weld metal, the cost of the steel is a major part of total costs. The expense of the high-toughness steels has not been found to be warranted for most building and bridges, whereas the cost of high-toughness filler metal is easily justifiable. Hot-rolled steels, which fracture in the transition region at the lowest service temperatures, have sufficient toughness for the required performance of most welded buildings and bridges.

24.3.1 Specification of Steel and Filler Metal

ASTM (American Society for Testing and Materials) specifications for bridge steel (A709) and ship steel (A131) provide for minimum CVN impact test energy levels. Structural steel specified by A36, A572, or A588, without supplemental specifications, does not require the Charpy test to be performed. If there is concern about brittle fracture and either (1) high ductility demand, (2) concern with low-temperature exposed structures, or (3) dynamic loading, then the CVN impact test should be specified

by the purchaser of steel as a supplemental requirement. The results of the CVN test, impact energies, are often referred to as "notch-toughness" values.

Because the Charpy test is relatively easy to perform, it will likely continue to be the measure of toughness used in steel specifications. In the range of temperatures called the brittle region, the Charpy notch toughness is approximately correlated with K_c from fracture mechanics tests. The CVN specification works by ensuring that the transition from brittle to ductile fracture occurs at some temperature less than service temperature. The notch toughness requirement ensures that brittle fracture will not occur as long as large cracks do not develop. Often 34 J (25 ft-lb), 27 J (20 ft-lb), or 20 J (15 ft-lb) are specified at a particular temperature. The intent of specifying any of these numbers is the same, i.e., to make sure that the transition starts below this temperature.

Charpy toughness requirements for steel and weld metal for bridges and buildings are compared in Table 24.2. This table is simplified and does not include all the requirements.

TABLE 24.2 Minimum Charpy Impact Test Requirements for Bridges and Buildings

	Minimum service temperature		
Material	−18°C Joules@°C	−34°C Joules@°C	−51°C Joules@°C
Steel: nonfracture critical members[a,b]	20@21	20@4	20@−12
Steel: fracture critical members[a,b]	34@21	34@4	34@−12
Weld metal for nonfracture critical[a]	27@−18	27@−18	27@−29
Weld metal for fracture critical[a,b]	34@−29°C for all service temperatures		
AISC: Jumbo sections and plates thicker than 50 mm[b]	27@21°C for all service temperature		

[a] These requirements are for welded steel with minimum specified yield strength up to 350 MPa up to 38 mm thick. Fracture critical members are defined as those that if fractured would result in collapse of the bridge.

[b] The requirements pertain only to members subjected to tension or tension due to bending.

Note that the bridge steel specifications require a CVN at a temperature 38°C *greater* than the minimum service temperature. This temperature shift accounts for the effect of strain rates, which are lower in the service loading of bridges (on the order of 10^{-3}) than in the Charpy test (greater than 10^{1}). It is possible to measure the toughness using a Charpy specimen loaded at a strain rate characteristic of bridges, called an intermediate strain rate, although the test is more difficult and the results are more variable. When the CVN energies from an intermediate strain rate are plotted as a function of temperature, the transition occurs at a temperature about 38°C lower for materials with yield strength up to 450 MPa.

As shown in Table 24.2, the AWS D1.5 *Bridge Welding Code* specifications for weld metal toughness are more demanding than the specifications for base metal. This is reasonable because the weld metal is always the location of discontinuities and high tensile residual stresses. However, there are no requirements for weld metal toughness in AWS D1.1. This lack of requirements was rationalized because typically the weld deposits are of higher toughness than the base metal. However, this is not always the case, e.g., the self-shielded flux-cored arc welds (FCAW-S) used in many of the WSMFs that fractured in the Northridge earthquake were reported to have very low toughness. The commentary in the AISC manual does warn that for "dynamic loading, the engineer may require the filler metals used to deliver notch-tough weld deposits".

ASTM A673 has specifications for the frequency of Charpy testing. The *H* frequency requires a set of three CVN specimens to be tested from one location for each heat or about 50 tons. These tests can be taken from a plate with thickness up to 9 mm different from the product thickness if it is rolled from the same heat. The P frequency requires a set of three specimens to be tested from one

end of every plate, or from one shape in every 15 tons of that shape. For bridge steel, the AASHTO code requires CVN tests at the H frequency as a minimum. For fracture critical members, the guide specifications require CVN testing at the P frequency. In the AISC code, CVN tests are required at the P frequency for thick plates and jumbo sections. A special test location in the core of the jumbo section is specified, as well as a requirement that the section tested be produced from the top of the ingot.

Even the P testing frequency may be insufficient for as-rolled structural steel. In a recent report for the National Cooperative Highway Research Program (NCHRP) [28], CVN data were obtained from various locations on bridge steel plates. The data showed that because of extreme variability in CVN across as-rolled plates, it would be possible to miss potentially brittle areas of plates if only one location per plate is sampled. For plates that were given a normalizing heat treatment, the excessive variability was eliminated.

24.3.2 Fracture Mechanics Analysis

Fracture mechanics is based on the mathematical analysis of solids with notches or cracks. Relationships between the material toughness, the crack size, and the stress or displacement will be derived below using fracture mechanics. The objective of a fracture mechanics analysis (as outlined herein) is to ensure that brittle fracture does not occur. Even if ductile fracture occurs before local buckling or another failure mode, ductile fracture is considered to give acceptable ductility. Brittle fracture occurs with nominal net-section stresses below or just slightly above the yield point. Therefore, the relatively simple principles of linear-elastic fracture mechanics (LEFM) can be used to conservatively assess whether a welded joint is likely to fail by brittle fracture rather than in a ductile manner.

It significantly simplifies the presentation and practical use of fracture mechanics if the discussion is confined to brittle fracture only. Worst-case assumptions are made regarding numerous factors that can enhance fracture toughness, e.g., temperature, strain rate, constraint, and notch acuity or sharpness. These assumptions eliminate the need for extensive discussion of these effects.

If necessary, these effects can be considered and more advanced principles of fracture mechanics can be used to estimate the maximum monotonic or cyclic rotation before ductile tearing failure. Fracture mechanics can also be used to predict the subcritical propagation of cracks due to fatigue and/or stress-corrosion cracking that may precede fracture. In order to present a thorough discussion of the brittle fracture problem here, we cannot provide a detailed discussion of many other interesting fracture mechanics topics. There are several excellent books on fracture mechanics that cover these topics in detail [6, 9, 10].

Although cracks can be loaded by shear, experience shows that only the tensile stress normal to the crack is important in causing fatigue or fracture in steel structures. This tensile loading is referred to as Mode I. When the plane of the crack is not normal to the maximum principal stress, a crack that propagates subcritically or in a stable manner will generally turn as it extends, such that it becomes normal to the principal tensile stress. Therefore, it is typically recommended that a welding defect or crack-like notch that is not oriented normal to the primary stresses can be idealized as an equivalent crack with a size equal to the projection of the actual crack area on a plane that is normal to the primary stresses (see [12], for example).

Brittle fracture occurs with nominal net-section stresses below or just slightly above the yield point. Therefore, the relatively simple principles of LEFM can be used to conservatively assess whether a welded joint is likely to fail by brittle fracture rather than in a ductile manner. LEFM gives a relatively straightforward method for predicting fracture, based on a parameter called the stress-intensity factor (K), which characterizes the stresses at notches or cracks [31]. The applied K is determined by the size of the crack (or crack-like notch) and the nominal cross-section stress remote from the crack. Crack-like notches and weld defects are idealized as cracks, which include crack-like notches and weld defects as well. In the case of linear elasticity, the stress-intensity factor can be considered a measure of

the magnitude of the crack tip stress and strain fields. Solutions for the applied stress-intensity factor, K, for a variety of geometries can be found in handbooks [43, 49, 50, 52]. Most of the solutions are variations on standard test specimens that have been studied extensively. The following discussion presents a few useful solutions and examples of their application to welded joints.

In general, the applied stress-intensity factor is given as

$$K = F_c * F_s * F_w * F_g * \sigma\sqrt{\pi a} \tag{24.5}$$

where the F terms are modifiers on the order of 1.0, specifically:

F_c = the factor for the effect of crack shape
F_s = the factor, equal to 1.12, that is used if a crack originates at a free surface
F_w = a correction for finite-width, which is necessary because the basic solutions were generally derived for infinite or semi-infinite bodies
F_g = a factor for the effect of nonuniform stresses, such as bending stress gradient

An SCF is defined as the ratio of the peak stress near the stress raiser to the nominal cross-section stress remote from the stress raiser. SCFs are often used in fracture assessments when the crack is located near a stress raiser. For example, a crack may be located at a plate edge that is badly corroded. Any SCF would also be included in F_g.

The stress-intensity factor has the unusual units of MPa-m$^{1/2}$ or ksi-in.$^{1/2}$. The material fracture toughness is characterized in terms of the applied K at the onset of fracture in simplified small test specimens, called K "critical" or K_c. The fracture toughness (K_c) is considered a transferable material property; i.e., fracture of structural details is predicted if the value of the applied K in the detail exceeds K_c. Equation 24.5 relates the important factors that influence fracture: K_c represents the material, σ represents the design, and a represents the fabrication and inspection.

In this section, K_c is used as any type of critical K associated with a quasi-static strain rate, derived from any one of a variety of test methods. One measure of K_c is the plane-strain fracture toughness, which is given the special subscript "I" for plane strain, K_{Ic}. K_{Ic} must be measured in specimens that are very thick and approximate plane strain. If the fracture toughness is measured in an impact test, the special designation K_d is used, where the subscript "d" is for dynamic. In practice, K_c is often estimated from correlations with the result from a CVN test because the CVN is much cheaper to perform and requires less material than a fracture mechanics test, and all test laboratories are equipped for the CVN test. A widely accepted correlation for the lower shelf and lower transition region between K_d and CVN [9]:

$$K_d = 11.5 * \sqrt{CVN} \tag{24.6}$$

where CVN is given in joules and K_d is given in MPa-m$^{1/2}$. A different constant is used for English units. This correlation is used to construct the lower part of the curve for dynamic fracture toughness (K_d) as a function of temperature directly from the curve of CVN vs. temperature. There is a temperature shift between the intermediate load rate values of K_c and the impact load rate values of K_d that is approximately equal to the temperature shift that occurs for CVN data. Therefore, K_c values for structural steel are obtained by shifting the K_d curve to a temperature that is 38°C lower. However, for brittle materials there is essentially no temperature shift and therefore K_c is approximately equal to K_d.

Prior to the 1994 Northridge earthquake, the welds in the WSMF connections were commonly made with the FCAW-S process using an E7XT-4 weld wire. For the connections fractured in the Northridge earthquake that have been investigated so far, the weld metal CVN is plotted in Figure 24.11. The lower-bound impact energy is between 4 and 14 J for temperatures up to 50°C. If recommended weld procedures are followed, the fracture toughness increases slightly but remains inadequate.

The lower bounds of the CVN and K_c data for the E7XT-4 weld metal is similar to the lower bounds from other brittle materials, such as the core region of the jumbo sections shown in Figure 24.4. This similarity in the data suggests that a there may be a lower-bound value of the fracture toughness that

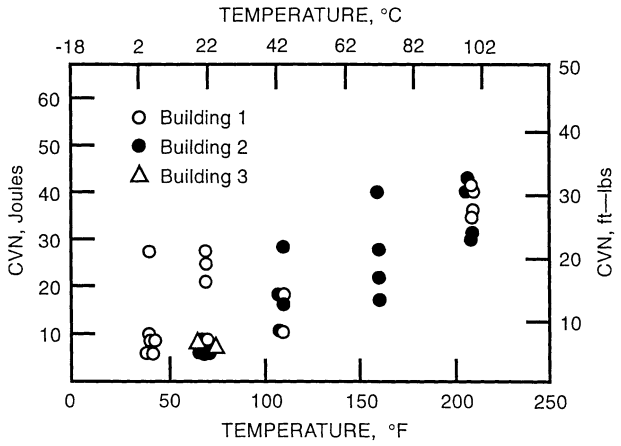

FIGURE 24.11: Typical Charpy impact energy from E7XT-4 self-shielded flux-cored arc welding weld metal from Northridge WSMF connections.

can be assumed for brittle ferritic weld metal, structural steel, and the heat-affected zone (HAZ). The lower-bound fracture toughness reflects the worst effects of temperature and strain rate. For these materials, the lower-bound fracture toughness was between 45 and 50 MPa-m$^{1/2}$. This concept of a lower-bound fracture toughness is very useful for fracture assessment.

As a consequence of the brittle fractures in jumbo sections, AISC specifications now have a supplemental Charpy requirement for shapes in groups 4 and 5 and (for the same reasons) plates greater than 51 mm thick, when these are welded and subject to primary tensile stress from axial load or bending. These jumbo shapes and thick plates must exhibit 27 J at 21°C. Using the correlation of Equation 24.6, 27 J will give a K_c of 60 MPa-m$^{1/2}$.

There are size and constraint effects and other complications that make the LEFM fracture toughness, K_c, less than perfect as a material property. This is especially true when K_c is estimated based only on a correlation to CVN. Nevertheless, as illustrated in the following, the conservative lower-bound value of K_c can be used by structural engineers to avoid brittle fracture.

Center Crack

The K solution for an infinitely wide plate with a through crack subject to uniform tensile membrane stress is

$$K = \sigma\sqrt{\pi a} \tag{24.7}$$

where

σ = nominal cross-section stress remote from the crack

$2a$ = the total overall crack length

If the total width of the panel is given as 2W, F_w for this crack geometry can be approximated by the Fedderson or secant formula:

$$F_w = \sqrt{\sec\frac{\pi a}{2W}} \tag{24.8}$$

This formula gives a value that is close to 1.0 and can be ignored for a/W less than a third. For a/W of about 0.5, the secant formula gives F_w of about 1.2. However, the values from the secant equation go to infinity as a approaches W. The secant formula is reasonably accurate for a/W up to 0.85. The F_w may be used for other crack geometries as well.

Many common buried defects and notches in welded joints can be idealized as a center crack in tension. For example, Figure 24.12 shows a backing bar with a fillet that is idealized as a center crack. The unfused area of the backing bar creates a crack-like notch with one tip in the root of the fillet

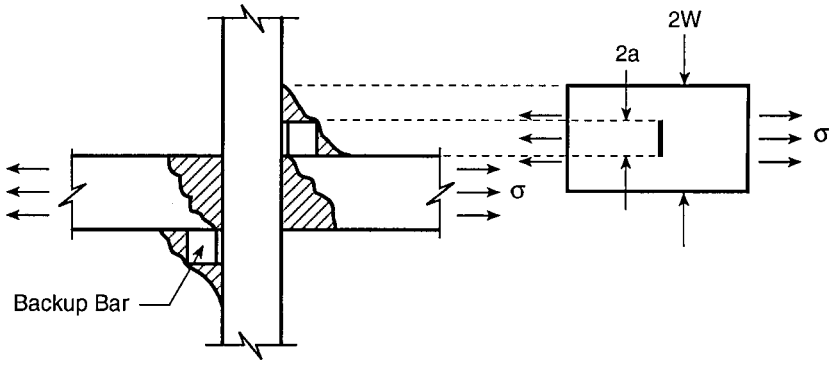

FIGURE 24.12: Cross-section of a one-sided groove-welded cruciform-type connection with loaded plate discontinuous and idealization of the notches from a backing bar with a fillet weld as a center-cracked tension panel.

weld and one tip at the root of the groove weld. The crack is asymmetrical but since the connection is subjected to uniform tension, the crack can be analyzed as if it were in a symmetric center-cracked panel. Of course, the applied K is higher on the crack tip that is in the root of the fillet weld because there is a high F_w for this side. Assuming the weld metal of the groove weld and the fillet weld have comparable toughness, the fillet weld side of the backing bar will govern the fracture limit state. Therefore, the panel is idealized as being symmetric with respect to the center of the backing bar.

Assuming negligible weld root penetration, the crack size ($2a$) is taken as being equal to the backing bar thickness, say 13 mm. For a/W of 0.5, Equation 24.8 gives F_w equal to 1.2. Although this idealization seems like a gross approximation at best, the validity of the K solution for this particular weld joint was verified based on observed fatigue crack propagation rates.

If this is a grade 50 steel, the yield strength could be up to 450 MPa. The notch tip could be subjected to full tensile residual stress. Therefore, Equation 24.5 is solved with the cross-section stress equal to 450 MPa, with the F_w factor of 1.2, and a of 6 mm, giving 74 MPa-m$^{1/2}$. It can be seen that this configuration could cause a brittle fracture for very brittle materials. However, weld metal and base steel with modest toughness could easily withstand this defect.

Edge Crack

The stress-intensity factor for an edge crack in an infinitely wide plate is

$$K = 1.12\sigma\sqrt{\pi a} \tag{24.9}$$

where σ is the remote cross-section nominal stress and a is the depth of the edge crack or crack-like notch. It can be seen that the edge crack equation is treated like half of a center crack, i.e., Equation 24.7, where a and W are the total length and width, respectively, for the edge crack. The F_s of 1.12 is applied to account for the free edge, which is not restrained as it is in the center-cracked geometry. Equation 24.9 is also modified with the F_w as in Equation 24.8.

Figure 24.5 showed a cross-section near the crack origin for a WSMF beam-flange-to-column weld that fractured in the Northridge earthquake. The fracture surfaces, such as shown in Figure 24.13,

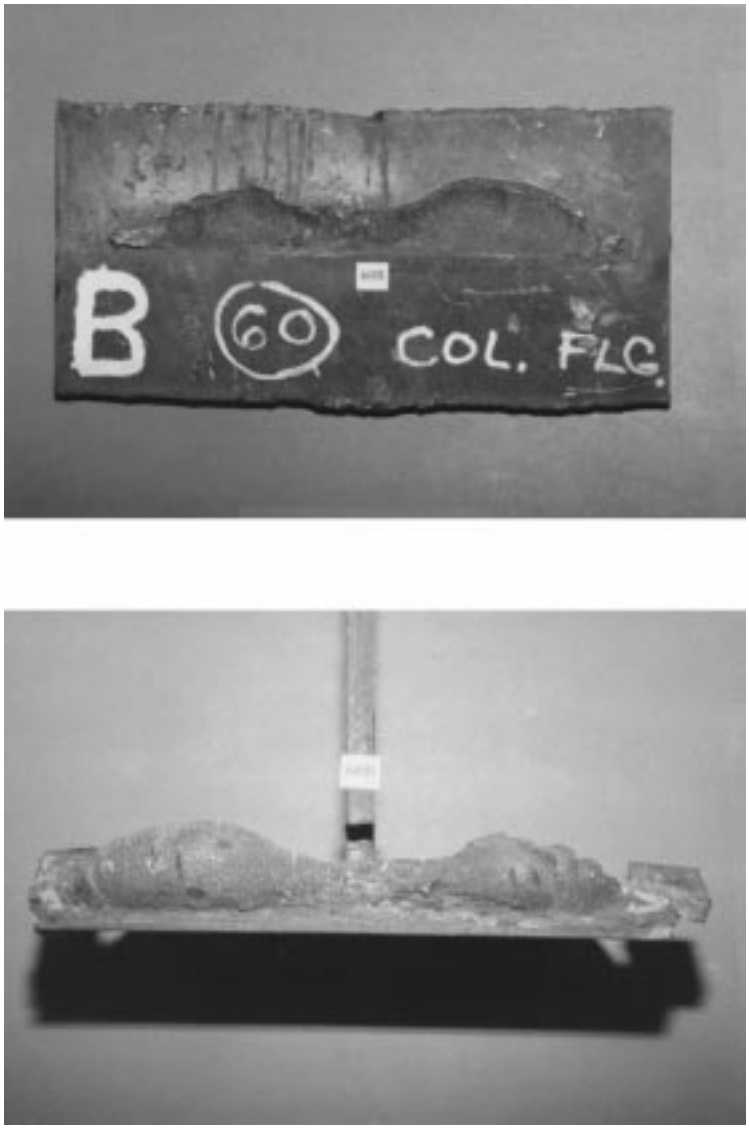

FIGURE 24.13: Fracture surfaces of a typical beam-flange-to-column joint of a WSMF that fractured in the Northridge earthquake, showing the lack-of-fusion defect in the center of the weld.

indicate that the fractures originate in the root of the weld, typically at a lack-of-fusion defect. This lack-of-fusion defect is difficult to avoid when the weld must be stopped on one side of the web and started on the other side. The weld fracture surface in Figure 24.13 shows the crack-like notch formed by the combination of a lack-of-fusion defect and the unfused edge of the backing bar. On a cross-section at the deepest point of the lack-of-fusion defect, the total depth of the notch, including the unfused edge of the backing bar, is from 13 to 19 mm.

The value of 45 MPa-$m^{1/2}$ can be used as a lower bound to the fracture toughness of structural steel or weld metal. Equation 24.9 may be used to predict brittle fracture for the WSMF connection welds when K exceeds 45 MPa-$m^{1/2}$. For a notch depth of 13 to 19 mm, Equation 24.9 would predict that brittle fracture is likely to occur for cross-section stress between 160 and 200 MPa, well below

the yield point. These types of LEFM calculations, had they been performed prior to the earthquake, would have predicted that brittle fracture would occur in the WSMF connections before yielding.

The propagation path of the unstable dynamic crack is seemingly chaotic, as it is influenced by dynamic stress waves and complex residual stress fields. The critical event was the initiation of the unstable crack in the brittle weld. There is little significance to whether the crack propagated in the weld or turned and entered the column.

The solution to the WSMF cracking problem is elimination of the possibility of such large defects (i.e., $\approx$ 19 mm) that result from the backing bar and any lack-of-fusion defect. The backing bar removal and back gouging to minimize the lack of fusion will eliminate most large crack-like conditions. However, this is not enough to eliminate the problem of brittle fracture. Appropriate weld notch toughness requirements must be specified to avoid the use of low-toughness weld metal.

There are certainly many other equally important design issues that influenced these fractures. The overall lack of redundancy, i.e., the reliance on only one or two massive WSMFs to resist lateral load in each direction, contributes to large forces and increases the thickness of the members and the high constraint of the connections. Even if brittle fracture is avoided, welds will typically fail at a lower level of plastic strain than base metal. Therefore, it can also be argued that it is imprudent to rely on welds for extensive plastic deformation. Several improved WSMF connections have been proposed, most of which are designed such that the plastic hinge develops in the span away from the connection. Nevertheless, in the event of unexpected loading, it is still desirable that these weld joints have a ductile failure mode. Therefore, while these improved connection designs may be worthwhile, the low-toughness weld metal and joint design with a built-in notch should still not be used under most circumstances.

Buried Penny-Shaped Crack

Many internal weld defects are idealized as an ellipse or a circle that is circumscribed around the projection of the weld defect on a plane perpendicular to the stresses. Often, the increased accuracy accrued by using the relatively complex elliptical formula is not worth the effort, and the circumscribed penny-shaped or circular crack is always conservative. The stress-intensity factor for the penny-shaped crack in an infinite body is given as

$$K = \frac{2}{\pi}\sigma\sqrt{\pi a} \tag{24.10}$$

where a is the radius of the circular crack. As for the other types of cracks, the F_w can be calculated using Equation 24.10. In terms of Equation 24.8, the crack shape factor F_c in this case is $2/\pi$ or 0.64. Using (1) the lower-bound fracture toughness of 45 MPa-m$^{1/2}$ and (2) an upper-bound residual stress plus applied stress equal to the upper-bound yield strength for grade 50 steel (450 MPa), Equation 24.10 shows that a penny-shaped crack would have to have a radius exceeding 8 mm to be critical, i.e., the diameter of the allowable welding defect would be 15 mm (providing that fatigue is not a potential problem).

The crack shape factor F_c is more favorable (0.64) for buried cracks as opposed to F_s of 1.12 for edge cracks, and the defect size is equal to $2a$ for the buried crack and only a for the edge crack. These factors explain why edge cracks of a given size are much more dangerous than buried cracks of the same size.

24.4 Summary

Structural elements for which the live load is a large percentage of the total load are potentially susceptible to fatigue. Many factors in fabrication can increase the potential for fatigue including notches, misalignment, and other geometrical discontinuities, thermal cutting, weld joint design

(particularly backing bars), residual stress, nondestructive evaluation and weld defects, intersecting welds, and inadequate weld access holes. The fatigue design procedures in the AASHTO and AISC specifications are based on control of the stress range and knowledge of the fatigue strength of the various details. Using these specifications, it is possible to identify and avoid details that are expected to have low fatigue strength.

Welded connections and thermal-cut hole copes, blocks, or cuts are potentially susceptible to brittle fracture. Many interrelated design variables can increase the potential for brittle fracture including lack of redundancy, large forces and moments with dynamic loading rates, thick members, geometrical discontinuities, and high constraint of the connections. Low temperature can be a factor for exposed structures. The factors mentioned above that influence the potential for fatigue have a similar effect on the potential for fracture. In addition, cold work, flame straightening, weld heat input, and weld sequence can also affect the potential for fracture. The AASHTO specifications [1] require a minimum CVN notch toughness at a specified temperature for the base metal and the weld metal of members loaded in tension or tension due to bending. Almost two decades of experience with these bridge specifications has proven that they are successful in significantly reducing the number of brittle fractures. Simple, LEFM concepts can be used to predict the potential for brittle fracture in buildings.

24.5 Defining Terms

a: Crack length.

A_t: The tensile stress area of a bolt.

AASHTO: American Association of State Highway Transportation Officials.

ACI: American Concrete Institute.

AISC: American Institute of Steel Construction.

ASTM: American Society for Testing and Materials.

AWS: American Welding Society.

BSI: British Standards Institute.

CAFL: Constant amplitude fatigue limit, a level of stress range below which noticeable cracking does not occur in constant amplitude fatigue tests.

CVN: Charpy V-Notch impact test energy.

d_b: The nominal diameter of a bolt (the body or shank diameter).

F_c: Factor for the effect of crack shape.

F_s: Factor, equal to 1.12, that is used if a crack originates at a free surface.

F_w: Correction for finite-width.

F_g: Factor for the effect of non-uniform stresses, such as bending stress gradient.

F_u: Ultimate tensile strength.

K: Stress-intensity factor.

K_c: Fracture toughness.

K_d: Dynamic fracture toughness.

L: Span length.

LFRD: Load and resistance factor design.

n: Threads per inch in bolts.

n_i: Number of cycles in an interval of stress range i.

N_{total}: Total number of stress ranges.

PTI: Post-Tensioning Institute.

$S_{\text{effective}}$: The effective stress range which is equal to the cube root of the mean cube of the all stress ranges.

S_i: Stress range for interval i.

SCF: Stress concentration factor.

t: Plate thickness.

g: Gage.

References

[1] American Association of State Highway Transportation Officials. 1994. *AASHTO LRFD Bridge Design Specifications,* First edition, Washington, D.C.

[2] American Concrete Institute Committee 215. 1996. Considerations for Design of Concrete Structures Subjected to Fatigue Loading, ACI 215R-74 (Revised 1992), *ACI Manual of Standard Practice,* Vol. 1.

[3] Ad-hoc Committee on Cable-Stayed Bridges. 1986. *Recommendations for Stay Cable Design and Testing,* Post-Tensioning Institute, Phoenix, AZ.

[4] American Institute of Steel Construction. 1994. *Load and Resistance Factor Design Specification for Structural Steel Buildings,* Second edition, Chicago, IL.

[5] American Petroleum Institute. 1989. *Recommended Practice for Planning, Designing, and Constructing Fixed Offshore Platforms,* API RP2A, 18th edition.

[6] Anderson, T.L. 1995. *Fracture Mechanics—Fundamentals and Applications,* Second edition, CRC Press, Boca Raton, FL.

[7] American Welding Society. 1996. *Structural Welding Code—Steel,* ANSI/AWS D1.1, Miami, FL.

[8] Ballio, G. and Castiglioni, C.A. 1994. A Unified Approach for the Design of Steel Structures Under Low and/or High Cycle Fatigue, *J. Constructional Steel Res.*

[9] Barsom, J.M. and Rolfe, S.T. 1987. *Fracture and Fatigue Control in Structures,* Second edition, Prentice-Hall, Englewood Cliffs, NJ.

[10] Broek, D. 1987. *Elementary Fracture Mechanics,* Fourth edition, Martinus Nijhoff Publishers, Dordrecht, the Netherlands.

[11] British Standards Institute. 1994. *Code of Practice for Fatigue Design and Assessment of Steel Structures,* BS 7608, London.

[12] British Standards Institute. 1991. *Guidance on Some Methods for the Derivation of Acceptance Levels for Defects in Fusion Welded Joints,* BSI PD 6493, London.

[13] Castiglioni, C.A. 1995. Cumulative Damage Assessment in Structural Steel Details, *Extending the Lifespan of Structures,* IABSE Symposium, San Francisco, CA, pp. 1061-1066.

[14] Demers, C. and Fisher, J.W. 1990. *Fatigue Cracking of Steel Bridge Structures, Volume I: A Survey of Localized Cracking in Steel Bridges—1981 to 1988,* Report No. FHWA-RD-89-166; *Volume II, A Commentary and Guide for Design, Evaluation, and Investigating Cracking,* Report No. FHWA-RD-89-167, Federal Highway Administration, McLean, VA.

[15] Dexter, R.J., Fisher, J.W., and Beach, J.E. 1993. Fatigue Behavior of Welded HSLA-80 Members, *Proceedings, 12th International Conference on Offshore Mechanics and Arctic Engineering,* Vol. III, Part A, Materials Engineering, American Society of Mechanical Engineers, New York, pp. 493-502.

[16] Dexter, R.J., Tarquinio, J.E., and Fisher, J.W. 1994. An Application of Hot-Spot Stress Fatigue Analysis to Attachments on Flexible Plate, *Proceedings of the 13th International Conference*

on Offshore Mechanics and Arctic Engineering, American Society of Mechanical Engineers, New York.

[17] Djikstra, O.D., Wardenier, J., and Hertogs, A.A. 1988. The Fatigue Behavior of Welded Splices With and Without Mouse Holes in IPE 400 and HEM 320 Beams, *Proceedings of the International Conference on Weld Failures—Weldtech '88,* The Welding Institute, Abington Hall, Cambridge, U.K.

[18] European Committee for Standardization. 1992. *Eurocode 3: Design of Steel Structures—Part 1.1: General Rules and Rules for Buildings,* ENV 1993-1-1, Brussels.

[19] Fisher, J.W. 1984. *Fatigue and Fracture in Steel Bridges,* ISBNO-471-80469-X, John Wiley & Sons, New York.

[20] Fisher, J.W., Frank, K.H., Hirt, M.A., and McNamee, B.M. 1970. *Effect of Weldments on the Fatigue Strength of Steel Beams,* National Cooperative Highway Research Program Report 102, Highway Research Board, Washington, D.C.

[21] Fisher, J.W., Albrecht, P.A., Yen, B.T., Klingerman, D.J., and McNamee, B.M. 1974. *Fatigue Strength of Steel Beams with Welded Stiffeners and Attachments,* National Cooperative Highway Research Program Report 147, Transportation Research Board, Washington, D.C.

[22] Fisher, J.W. and Pense, A.W. 1987. Experience with Use of Heavy W Shapes in Tension, *Eng. J.,* American Institute of Steel Construction, 24(2).

[23] Fisher, J.W. and Keating, P.B. 1989. Distortion-Induced Fatigue Cracking of Bridge Details with Web Gaps, *J. Constructional Steel Res.,* (12), 215-228.

[24] Fisher, J.W., Jian, J., Wagner, D.C., and Yen, B.T. 1990. *Distortion-Induced Fatigue Cracking in Steel Bridges,* National Cooperative Highway Research Program Report 336, Transportation Research Board, Washington, D.C.

[25] Fisher, J.W., et al. 1993. *Resistance of Welded Details Under Variable Amplitude Long-Life Fatigue Loading,* National Cooperative Highway Research Program Report 354, Transportation Research Board, Washington, D.C.

[26] Frank, K.H. and Fisher, J.W. 1979. Fatigue Strength of Fillet Welded Cruciform Joints, *J. Structural Div.,* ASCE, 105(ST9), 1727-1740.

[27] Frank, K.H. 1980. Fatigue Strength of Anchor Bolts, *J. Structural Div.,* ASCE, 106 (ST).

[28] Frank, K.H., et al. 1993. *Notch Toughness Variability in Bridge Steel Plates,* National Cooperative Highway Research Program Report 355, Washington, D.C.

[29] American Association of State Highway and Transportation Officials. 1978. *Guide Specifications for Fracture Critical Non-Redundant Steel Bridge Members,* Washington, D.C.

[30] Hahin, C. 1994. *Effects of Corrosion and Fatigue on the Load-Carrying Capacity of Structural Steel and Reinforcing Steel,* Illinois Physical Research Report No. 108, Illinois Department of Transportation, Springfield, IL.

[31] Irwin, G.R. 1957. Analysis of Stresses and Strains Near the End of Crack Traversing a Plate, *Trans., ASME, J. Appl. Mech.,* Vol. 24. Also reprinted in ASTM volume on classic papers.

[32] Kaczinski, M.R., Dexter, R.J., and Van Dien, J.P. 1996. *Fatigue-Resistant Design of Cantilevered Signal, Sign, and Light Supports,* Final Report for NCHRP Project 10-38, ATLSS Engineering Research Center, Lehigh University.

[33] Kaufmann, E.J., Xue, M., Lu, L.-W., and Fisher, J.W. 1996. Achieving Ductile Behavior of Moment Connections, *Modern Steel Construction,* 36(1), 30-39.

[34] Keating, P.B. and Fisher, J.W. 1986. *Evaluation of Fatigue Tests and Design Criteria on Welded Details,* National Cooperative Highway Research Program, Report 286, Washington, D.C.

[35] Kober, Dexter, R.J., Kaufmann, E.J., Yen, B.T., and Fisher, J.W. 1994. The Effect of Welding Discontinuities on the Variability of Fatigue Life, *Fracture Mech.,* Twenty-Fifth Volume, ASTM STP 1220, F. Erdogan and Ronald J. Hartranft, Eds., American Society for Testing and Materials, Philadelphia, PA.

[36] Krawinkler, H. and Zohrei, M. 1983. Cumulative Damage in Steel Structures Subjected to Earthquake Ground Motion, *Computers and Structures,* 16(1-4), 531-541.
[37] Kulak, G.L., Fisher, J.W., and Struick, J.H. 1987. *Guide to Design Criteria for Bolted and Riveted Joints*, Second Edition, Prentice-Hall, Englewood Cliffs, NJ.
[38] Maddox, S.J. 1991. *Fatigue Strength of Welded Structures,* Second Edition, Abington Publishing, Cambridge, UK.
[39] Marsh, K.J., Ed. 1988. *Full-Scale Fatigue Testing of Components and Structures,* Butterworths, London.
[40] Marshall, P.W. 1992. *Design of Welded Tubular Connections,* Elsevier, New York.
[41] Miki, C., Nishimura, T., Tajima, J., and Okukawa, A. 1980. Fatigue Strength of Steel Members Having Longitudinal Single-Bevel Groove Welds, *Trans. Japan Weld. Soc.,* 11(1), 43-56.
[42] Miner, M.A. 1945. Cumulative Damage in Fatigue, *J. Appl. Mech.,* 12, A-159.
[43] Murakami, Y., et al., Eds. 1987. *Stress Intensity Factors Handbook,* Vols. 1 and 2, Pergamon Press, Oxford, U.K.
[44] Outt, J.M.M., Fisher, J.W., and Yen, B.T. 1984. *Fatigue Strength of Weathered and Deteriorated Riveted Members,* Report DOT/OST/P-34/85/016, Department of Transportation, Federal Highway Administration, Washington, D.C.
[45] Overnman, T.R., Breen, J.E., and Frank, K.H. 1984. *Fatigue Behavior of Pretensioned Concrete Girders,* Research Report 300-2F, Center for Transportation Research, The University of Texas at Austin.
[46] Petershagen, H. 1986. Fatigue Problems in Ship Structures, *Advances in Marine Structures,* Elsevier Applied Science, London, pp. 281-304.
[47] Pfister, J.F. and Hognestad, E. 1964. High Strength Bars as Concrete Reinforcement, Part 6, Fatigue Tests, *J. PCA Res. Dev. Lab.,* 6(1), 65-84.
[48] Rabbat, B.G., et al. 1979. Fatigue Tests of Pretensioned Girders with Blanketed and Draped Strands, *J. Prestressed Concrete Inst.,* 24(4), 88-115.
[49] Rooke, D.P. and Cartwright, D.J. 1974. *Compendium of Stress Intensity Factors,* Her Majesty's Stationery Office, London.
[50] Rooke, D.P. 1986. *Compounding Stress Intensity Factors,* Research Reports in Materials Science (Series One), The Parthenon Press, Lancashire, U.K.
[51] Sternberg, F. 1969. *Performance of Continuously Reinforced Concrete Pavement, I-84 Southington,* Connecticut State Highway Department.
[52] Tada, H. 1985. *The Stress Analysis of Cracks Handbook,* Paris Productions, Inc., St. Louis, MO.
[53] Tide, R.H.R., Fisher, J.W., and Kaufmann, E.J. 1996. Substandard Welding Quality Exposed: Northridge, California Earthquake, January 17, 1994, IIW Asian Pacific Welding Congress, Auckland, New Zealand, February 4-9.
[54] VanDien, J.P., Kaczinski, M.R., and Dexter, R.J. 1996. Fatigue Testing of Anchor Bolts, *Building an International Community of Structural Engineers,* Vol. 1, Proceedings of Structures Congress XIV, Chicago, pp. 337-344.
[55] Xue, M., Kaufmann, E.J., Lu, L.W., and Fisher, J.W. 1996. Achieving Ductile Behavior of Moment Connections—Part II, *Modern Steel Construction,* 36(6), 38-42.
[56] Yagi, J., Machida, S., Tomita, Y., Matoba, M., and Kawasaki, T. 1991. *Definition of Hot-Spot Stress in Welded Plate Type Structure for Fatigue Assessment,* International Institute of Welding, IIW-XIII-1414-91.
[57] Yen, B.T., Huang, T., Lai, L.Y., and Fisher, J.W. 1990. *Manual for Inspecting Bridges for Fatigue Damage Conditions,* Report No. FHWA-PA-89-022 + 85-02, Fritz Engineering Laboratory Report No. 511.1, Pennsylvania Department of Transportation, Harrisburg, PA.
[58] Yen, B.T., et al. 1991. Fatigue Behavior of Stringer-Floorbeam Connections, *Proceedings of the Eighth International Bridge Conference,* IBC-91-19, Engineers' Society of Western Pennsylvania, pp. 149-155.

Further Reading

[1] Anderson, T.L. 1995. *Fracture Mechanics — Fundamentals and Applications,* 2nd ed., CRC Press, Boca Raton, FL.

[2] Barsom, J.M. and Rolfe, S.T. 1987. *Fracture and Fatigue Control in Structures,* 2nd ed., Prentice-Hall, Englewood Cliffs, NJ.

[3] Broek, D. 1987. *Elementary Fracture Mechanics,* 4th ed., Martinus Nijhoff Publishers, Dordrecht, Netherlands.

[4] Fisher, J.W. 1984. *Fatigue and Fracture in Steel Bridges,* John Wiley & Sons, New York.

[5] Maddox, S.J. 1991. *Fatigue Strength of Welded Structures,* 2nd ed., Abington Publishing, Cambridge, U.K.